

# Spectroscopic and photophysical responses of a ruthenium(II) dication–calix[4]arenetetrasulfonate hybrid complex upon ion binding

Masahiro Chiba, Haeng-Boo Kim<sup>1</sup>, Noboru Kitamura\*

Division of Chemistry, Graduate School of Science, Hokkaido University, Sapporo 060-0810, Japan

Received 5 November 2001; received in revised form 15 January 2002; accepted 25 January 2002

## Abstract

A  $\text{CS}^{4-}:(\text{RuB}_3^{2+})_2$  hybrid complex as a new class of a chemosensor was prepared by an ion-exchange reaction, where  $\text{CS}^{4-}$  and  $\text{RuB}_3^{2+}$  were calix[4]arenetetrasulfonate and a tris(2,2'-bipyridine)ruthenium(II) dication, respectively. In the solid state, one  $\text{RuB}_3^{2+}$  was shown to bury partly in the cavity of  $\text{CS}^{4-}$  from the upper rim, while other  $\text{RuB}_3^{2+}$  sits near the  $\text{CS}^{4-}:\text{RuB}_3^{2+}$  ion-pair to balance the total electric charge of the hybrid. In methanol, on the other hand, two  $\text{RuB}_3^{2+}$  molecules in the hybrid complex located in the vicinity of a  $\text{CS}^{4-}$  molecule at analogous microenvironments as suggested by  $^1\text{H-NMR}$ . Spectroscopic and excited-state properties of  $\text{RuB}_3^{2+}$  in the hybrid were influenced by  $\text{CS}^{4-}$  through the ion-excited dipole interaction and photoinduced electron transfer quenching. In the presence of a foreign cation as a guest, the emission intensity and lifetime of  $\text{RuB}_3^{2+}$  increased, demonstrating that  $\text{CS}^{4-}:(\text{RuB}_3^{2+})_2$  hybrid complex acted as a luminescent chemosensor. The mechanism of ion recognition was discussed in terms of changes in the photophysical properties of the hybrid complex. © 2002 Elsevier Science B.V. All rights reserved.

**Keywords:** Ru(II) complex; Photodynamics; Calix[4]arenetetrasulfonate; Chemosensor

## 1. Introduction

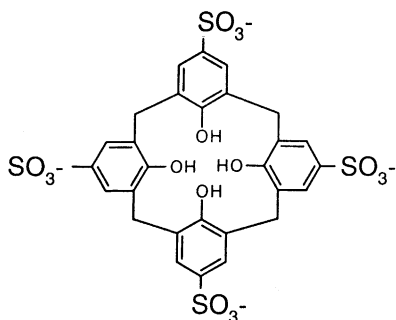
Calix[*n*]arenes are a very fascinating class of container molecules and their abilities towards ion/molecule recognition were studied extensively among the past decades [1,2]. As one of the spectroscopic properties, the compounds show UV absorption bands at around 280 and 288 nm due to the electronic transitions in the phenol groups. For photometric and/or fluorometric diagnosis of an ion or molecule by calix[*n*]arene, therefore, a spectroscopically active chromophore(s) should be introduced to the molecule, since calix[*n*]arenes themselves do not exhibit absorption and emission in the visible region. As an example, Beer et al. [3] reported calix[4]arene derivatives linked covalently with two tris(2,2'-bipyridine)ruthenium(II) chromophores ( $\text{RuB}_3^{2+}$ ), and demonstrated that the derivatives acted as luminescent chemosensors towards several anions: phosphate, halide, and so forth. Hasek et al. [4] also reported a calix[6]arene derivative having  $\text{RuB}_3^{2+}$  moieties as an anion sensor. Clearly, these challenging works are of primary

importance for further advances in spectroscopic diagnosis of various ions and molecules. Nonetheless, introduction of a spectroscopically active chromophore(s) to calix[*n*]arene requires sometimes laborious synthetic works.

In order to develop a more convenient approach to a spectroscopic chemosensor based on calix[*n*]arene, we focused our attention to calix[4]arenetetrasulfonate ( $\text{CS}^{4-}$ , Scheme 1), first prepared by Shinkai et al. [5]. We suppose that the counter cations ( $\text{Na}^+$ ) of  $\text{CS}^{4-}$  could be easily replaced by a cationic luminescent dye(s),  $\text{D}^{m+}$ , producing a  $\text{CS}^{4-}:\text{D}^{m+}$  ion-pair. If the spectroscopic and excited-state properties of the ion-pair itself or  $\text{D}^{m+}$  bound to  $\text{CS}^{4-}$  are under the influence of a foreign ion or molecule, the ion-pair would act as a chemosensor. Among various cationic dyes, we chose  $\text{RuB}_3^{2+}$ , since its spectroscopic and excited-state properties have been well-known [6] and the counter anions of  $\text{RuB}_3^{2+}$  can be readily replaced by various anions:  $\text{Cl}^-$ ,  $\text{ClO}_4^-$ ,  $\text{PF}_6^-$  and so forth. Furthermore, the spectroscopic properties of a structurally analogous complex of osmium(II) having 1,10-phenanthroline ligands have been reported to be sensitive to nature of the counter anions [7]. Therefore, we expected that a  $\text{CS}^{4-}:(\text{RuB}_3^{2+})_2$  hybrid complex could be used as a new class of a luminescent chemosensor. In this paper, we report preparation and characterization of the  $\text{CS}^{4-}:(\text{RuB}_3^{2+})_2$  hybrid complex, and its spectroscopic responses towards several cations are discussed.

\* Corresponding author. Tel.: +81-11-706-2697; fax: +81-11-706-2711.  
E-mail address: kitamura@sci.hokudai.ac.jp (N. Kitamura).

<sup>1</sup> Present address: Engineering Research Institute, Faculty of Engineering, The University of Tokyo, 2-11-16 Yayoi, Bunkyo-ku, Tokyo 113-8656, Japan.



Scheme 1. Chemical structure of calix[4]arenetetrasulfonate ( $\text{CS}^{4-}$ ).

## 2. Experimental

### 2.1. Chemicals

A calix[4]arenetetrasulfonic acid tetrasodium salt ( $\text{Na}^+_4\text{CS}^{4-}$ ), purchased from Sugai Chem., was used as received. Tris(2,2'-bipyridine)ruthenium(II) ( $\text{RuB}_3^{2+}$ ) as a chloride salt was purchased from Aldrich and was purified by repeated recrystallizations from an ethanol/diethyl ether. Inorganic salts ( $\text{NaClO}_4$ ,  $\text{Mg}(\text{ClO}_4)_2$  and  $\text{Al}(\text{ClO}_4)_3$ ) with the highest purities available from the suppliers (Kanto Chem., Aldrich, or Tokyo Kasei) were used without further purification. Tetra-*n*-butylammonium perchlorate ( $\text{Bu}_4\text{NClO}_4$ , Tokyo Kasei) was purified by repeated recrystallizations from an ethanol/diethyl ether mixture. Methanol (DOTITE, spectroscopic grade) and *N,N*-dimethylformamide (DMF, Kanto Chem., electrochemical analysis grade) were used as received. Water was used after deionization and distillation (Advantec Toyo, GSR-200).

### 2.2. Spectroscopic and electrochemical measurements

Steady-state absorption and emission spectroscopies were conducted by using a Hitachi U-3300 spectrophotometer and a Hitachi F-4500 spectrofluorometer, respectively. For nanosecond emission spectroscopy, the third harmonics from a pulsed Nd:YAG laser (355 nm, 4 ns pulse width, Surelite-2, Continuum) was used for excitation and the emission from a sample was analyzed by using a streak camera (C4334, Hamamatsu Photonics) equipped with a spectrograph (C5094, Hamamatsu Photonics). A timing between the laser and the detector was controlled by using a pulsed delay generator (DG535, Stanford Research Systems). For both steady-state and time-resolved emission spectroscopies, the temperature of a sample solution was controlled at 25 °C by circulating water to a sample holder with an electronic water circulator (FR-007, Fine or CTE-42A, Yamato-Komatsu). Electrochemical measurements were conducted by using an electrochemical analyzer (ALS-701A, ALS) with working, reference, and counter electrodes being Pt, SCE and Ag electrodes, respectively. As a supporting electrolyte, purified  $\text{Bu}_4\text{NClO}_4$  (50 mM) was used.

### 2.3. Other measurements

NMR spectroscopy was made with a 300 MHz Gemini-2000 spectrometer (Varian) by using methanol- $d_4$  (Wako Chem.) as a solvent. An X-ray crystallographic analysis of the ion-pair complex was conducted with a Mercury CCD detector coupled with a AFC-8S diffractometer (Rigaku).

## 3. Results and discussion

### 3.1. Preparation and characterization of $\text{CS}^{4-}$ : ( $\text{RuB}_3^{2+}$ )<sub>2</sub> hybrid complex

An ion-pair complex between  $\text{CS}^{4-}$  and  $\text{RuB}_3^{2+}$  was easily prepared by adding an aqueous  $\text{RuB}_3^{2+}\text{Cl}^-_2$  solution (>2 eq.) to an aqueous solution of  $\text{Na}^+_4\text{CS}^{4-}$ , by which the ion-pair complex was obtained as red precipitates. After thorough washing with pure water, the ion-pair complex was purified by repeated recrystallizations from methanol. An elementary analysis of the hybrid complex demonstrated that the mole ratio of  $\text{CS}^{4-}$  to  $\text{RuB}_3^{2+}$  was 1:2,<sup>2</sup> indicating that two  $\text{RuB}_3^{2+}$  molecules were bound to one  $\text{CS}^{4-}$  molecule:  $\text{CS}^{4-}:(\text{RuB}_3^{2+})_2$ . The results are very reasonable as expected from the total electric charges of  $\text{CS}^{4-}$  and  $\text{RuB}_3^{2+}$ .

In order to obtain more detailed information about the structure of the hybrid complex, we conducted an X-ray structural analysis. Since crystalline water molecules in the hybrid were lost during the experiments, the *R* and *R<sub>w</sub>* values were somewhat large.<sup>3</sup> Thus, we cannot discuss detailed structural parameters at the present stage of the investigation: bond lengths, bond angles and so forth. However, we succeeded in obtaining information about the characteristic overall structure of the hybrid as shown in Fig. 1. As expected from the results by the elemental analysis, the hybrid was shown to be composed of one  $\text{CS}^{4-}$  and two  $\text{RuB}_3^{2+}$ . However, the microenvironments around two  $\text{RuB}_3^{2+}$  in the hybrid were different with each other. Namely, one  $\text{RuB}_3^{2+}$  molecule is buried partly into the cavity of  $\text{CS}^{4-}$  from the upper rim (Fig. 1a), while other  $\text{RuB}_3^{2+}$  sits very closely to the  $\text{CS}^{4-}:\text{RuB}_3^{2+}$  one-to-one ion-pair to balance the total electric charge of the hybrid (Fig. 1b). In the solid state, therefore, the hybrid complex possesses very unique structures. In methanol, on the other hand, the <sup>1</sup>H-NMR spectrum of the hybrid complex suggests that two  $\text{RuB}_3^{2+}$  located near a  $\text{CS}^{4-}$  molecule at analogous microenvironments, since the proton signals

<sup>2</sup>  $\text{C}_{88}\text{H}_{68}\text{N}_{12}\text{O}_{16}\text{S}_4\text{Ru}_2 \cdot 4(\text{H}_2\text{O})$ : Found (Calc.): C, 54.00 (54.15); H, 4.18 (3.92); N, 8.59 (8.61); S, 6.57 (6.57).

<sup>3</sup> Structure determination of  $(\text{Ru}(\text{B})_3^{2+})_2(\text{CS}^{4-})(\text{C}_{88}\text{H}_{68}\text{N}_{12}\text{O}_{16}\text{S}_4\text{Ru}_2)$ : triclinic, space group P-1 (No. 2), *a* = 16.965(5) Å, *b* = 18.367(3) Å, *c* = 19.647(5) Å,  $\alpha$  = 62.092(8)°,  $\beta$  = 86.987(8)°,  $\gamma$  = 76.632(7)°, *V* = 5252.758(3) Å<sup>3</sup>. The number of total reflections collected was 10551. Final *R* and *R<sub>w</sub>* values were 0.132 and 0.154, respectively, for 1196 valuable parameters.

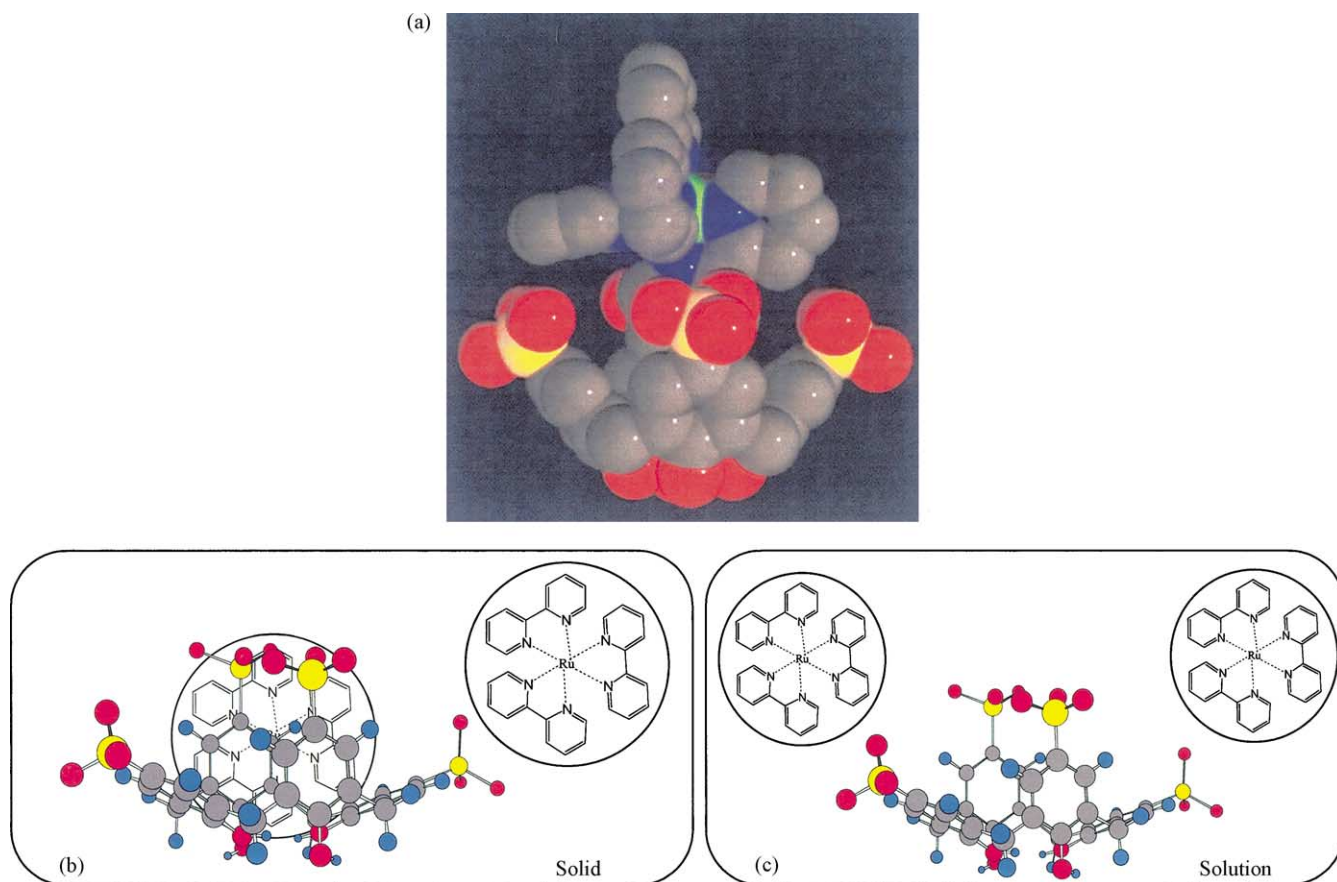


Fig. 1. Predicted structures of a  $CS^{4-}:(RuB_3^{2+})_2$  hybrid complex. A  $CS^{4-}:(RuB_3^{2+})$  ion-pair in the solid state (a) and the overall structures of the hybrid complex predicted from X-ray crystallography (b). The structures in solution predicted from  $^1H$ -NMR (c).

responsible for the 2,2'-bipyridine ligands did not split into those of each  $RuB_3^{2+}$  molecule (data are not shown here). In solution, therefore, we suppose that the hybrid complex is solubilized as shown schematically in Fig. 1c.

### 3.2. Spectroscopic and excited-state properties of $CS^{4-}:(RuB_3^{2+})_2$ hybrid complex

Fig. 2 shows absorption and emission (uncorrected, excited at 355 nm) spectra of the hybrid complex in methanol. The absorption spectrum exhibits metal-to-ligand charge transfer (MLCT) and ligand-centered (LC) bands at around 452 and 288 nm, respectively, which agrees very well with those of  $RuB_3^{2+}(PF_6^-)_2$  [6]. Knowing the composition of the hybrid complex to be  $CS^{4-}:(RuB_3^{2+})_2$ , the molar absorptivity of the MLCT band was calculated to be  $2.1 \times 10^4 M^{-1} cm^{-1}$ , which was almost two times larger than that of  $RuB_3^{2+}(PF_6^-)_2$  ( $1.4 \times 10^4 M^{-1} cm^{-1}$ ). On the other hand, although the emission spectral band shape of the hybrid complex was very similar to that of  $RuB_3^{2+}$ , the maximum wavelength of the hybrid was shifted slightly to the red (615 nm) as compared to that of  $RuB_3^{2+}(PF_6^-)_2$  (610 nm). Furthermore, the emission quantum yield of the hybrid complex (0.045, deaerated) was slightly lower than

that of  $RuB_3^{2+}(PF_6^-)_2$  (0.051). Although the absorption characteristics of  $RuB_3^{2+}$  in the hybrid were insensitive to the sulfonate groups in  $CS^{4-}$ , the excited-state properties of  $RuB_3^{2+}$  were shown to be certainly influenced by nature of the counter anions.

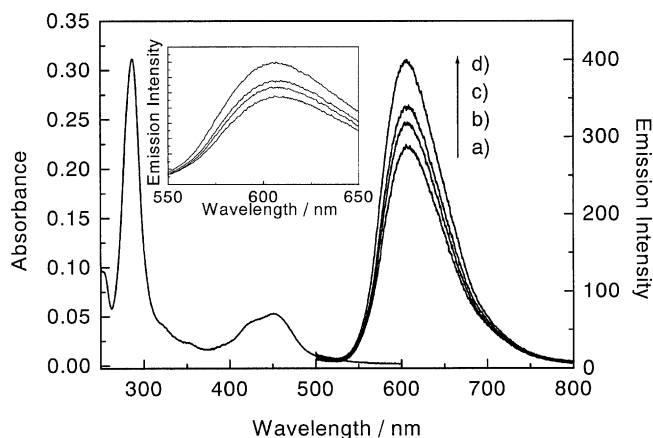


Fig. 2. Absorption and emission spectra (a) of a  $CS^{4-}:(RuB_3^{2+})_2$  hybrid complex ( $2.2 \times 10^{-6} M$ ) in methanol and the emission intensity responses of the hybrid by  $NaClO_4$  (b:  $1.3 \times 10^{-4}$ , c:  $1.3 \times 10^{-3}$ , d:  $1.3 \times 10^{-2} M$ ). Excitation wavelength is 355 nm.

For osmium(II) complexes having 1,10-phenanthroline derivatives ( $\text{Os}(\text{phen})_3^{2+}$ ), Vinning et al. [7] reported the effects of the counter anions on the emission maximum wavelength ( $\lambda_{\text{max}}^{\text{em}}$ ) and the non-radiative decay rate constant ( $k_{\text{nr}}$ ) of the complex, and demonstrated that the increase in the counter anion size brought about a red shift of  $\lambda_{\text{max}}^{\text{em}}$  and an increase in  $k_{\text{nr}}$ . In the MLCT excited state of  $\text{RuB}_3^{2+}$  or  $\text{Os}(\text{phen})_3^{2+}$ , it is well-known that the excited electron is localized on a single ligand [8] in a short time scale and this causes a relatively large excited-state dipole moment:  $14 \pm 6$  or  $13 \pm 6$  D for  $\text{RuB}_3^{2+}$  or  $\text{Os}(\text{phen})_3^{2+}$ , respectively. Therefore, they concluded that the counter anion-dipole (i.e., excited-state dipole) interaction was one of the origins of the counter anion effects on  $\lambda_{\text{max}}^{\text{em}}$  and  $k_{\text{nr}}$  of  $\text{Os}(\text{phen})_3^{2+}$ . In the MLCT excited state with a  $C_2$  symmetry, furthermore, the counter anions would be likely to locate the opposite sites to an electron-localized ligand due to electrostatic repulsion, while this is not the case in the ground state ( $D_3$  symmetry). Therefore, such situations lead to the difference in the ground- and excited-state energies (i.e.,  $\lambda_{\text{max}}^{\text{em}}$ ) with nature of the counter anions. In the present case, since  $\text{RuB}_3^{2+}$  in the hybrid complex is under the strong influence of the electrostatic field by  $\text{CS}^{4-}$  as a counter anion, the red shift of  $\lambda_{\text{max}}^{\text{em}}$  compared to  $\lambda_{\text{max}}^{\text{em}}$  of  $\text{RuB}_3^{2+}(\text{PF}_6^-)_2$  will be explained by the analogous context with those described above.

The above discussion indicates that the emission lifetime ( $\tau$ ) or  $k_{\text{nr}}$  of  $\text{RuB}_3^{2+}$  in the hybrid complex should be shorter or larger than that of  $\text{RuB}_3^{2+}(\text{PF}_6^-)_2$ , respectively. Therefore, we conducted emission decay measurements of the hybrid complex in a deaerated methanol as the data were shown in Fig. 3. Although it is not clear enough from the figure (a), the emission decay was not fitted by a single exponential function, while that was analyzed successfully by two time constants (390 and 720 ns) with chi-squared and Durbin–Watson parameters being 1.01 and 1.85, respectively. The long lifetime component ( $\tau_1 = 720$  ns) observed

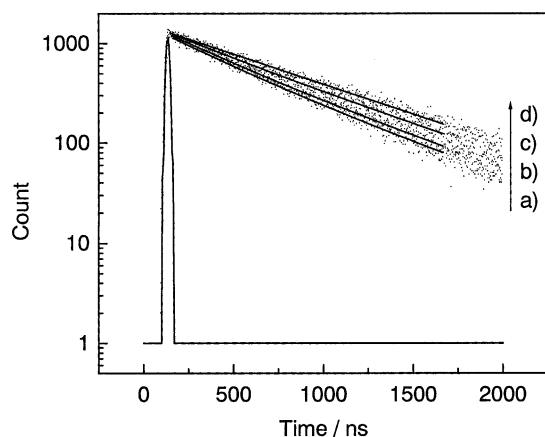


Fig. 3. Emission decay profiles of a  $\text{CS}^{4-}:(\text{RuB}_3^{2+})_2$  hybrid complex ( $2.2 \times 10^{-6}$  M) in the absence (a) and presence of  $\text{NaClO}_4$  (b:  $2.5 \times 10^{-5}$ , c:  $1.3 \times 10^{-4}$ , d:  $1.3 \times 10^{-2}$  M) in methanol (deaerated). Excitation and emission monitor wavelengths were set at 355 and 610 nm, respectively. A sharp time response profile represents an instrumental response.

in the hybrid agreed very well with that of  $\text{RuB}_3^{2+}(\text{PF}_6^-)_2$  in methanol. Therefore, one  $\text{RuB}_3^{2+}$  molecule in the hybrid is concluded to be free from the interactions with  $\text{CS}^{4-}$ , probably due to the association–dissociation equilibrium of the ion-pair in methanol, though we have not determined the equilibrium constant. On the other hand, the short decay component ( $\tau_s = 390$  ns) will be best ascribed to  $\text{RuB}_3^{2+}$  interacted with  $\text{CS}^{4-}$ . The emission showed a double-exponential decay, so that we could not determine the  $k_{\text{nr}}$  value for the hybrid. However, since the hybrid exhibited the red-shifted emission and the low emission quantum yield compared to those of  $\text{RuB}_3^{2+}(\text{PF}_6^-)_2$ , the  $k_{\text{nr}}$  value of the hybrid should be larger than that of  $\text{RuB}_3^{2+}(\text{PF}_6^-)_2$ , as expected from the energy gap law [9]. Therefore, the excited-state properties of  $\text{RuB}_3^{2+}$  in the hybrid are concluded to be under the strong influence of  $\text{CS}^{4-}$ .

However, the  $\tau_s$  value of 390 ns is apparently too short to explain the results by the ion–dipole interactions alone, including electrostatic repulsion between  $\text{CS}^{4-}$  and the electron-localized ligand. In order to check further a possibility of a direct electronic interaction between  $\text{RuB}_3^{2+}$  and  $\text{CS}^{4-}$ , we conducted emission quenching experiments of  $\text{RuB}_3^{2+}(\text{Cl}^-)_2$  by  $\text{CS}^{4-}$  in aqueous dilute solutions. In order to avoid ion-pair precipitation, the concentrations of the ions were set at  $[\text{RuB}_3^{2+}] = 8.0 \times 10^{-6}$  M and  $[\text{CS}^{4-}] < 1.5 \times 10^{-5}$  M in the experiments. Although ion-pair formation between  $\text{RuB}_3^{2+}$  and  $\text{CS}^{4-}$  participated to some extent even under the dilute conditions, the  $\text{RuB}_3^{2+}$  emission was certainly quenched by  $\text{CS}^{4-}$  with the apparent rate constant of  $\sim 7 \times 10^{10} \text{ M}^{-1} \text{ s}^{-1}$ . Furthermore, cyclic voltammetry of the hybrid complex in DMF indicates that a new oxidation peak appears at around 1.0 V (vs. SCE) in addition to the redox peaks responsible for  $\text{RuB}_3^{2+}$ . On the basis of the redox and excited-state parameters of both  $\text{RuB}_3^{2+}$  and  $\text{CS}^{4-}$ ,<sup>4</sup> the Gibbs free energy change for photoinduced electron transfer (PET) quenching of  $\text{RuB}_3^{2+}$  by  $\text{CS}^{4-}$  was estimated to be +0.4 kcal/mol. Although the value is not exothermic enough, PET quenching will be likely to proceed when  $\text{RuB}_3^{2+}$  is bound to  $\text{CS}^{4-}$  in methanol. Therefore, we conclude that the short excited-state lifetime component observed for the hybrid ( $\tau_s = 390$  ns) is ascribable to both the ion–dipole interaction and PET quenching. If these quenching mechanisms are influenced by a foreign ion, the hybrid complex would act as a new spectroscopic sensor.

### 3.3. Spectroscopic responses of $\text{CS}^{4-}:(\text{RuB}_3^{2+})_2$ hybrid complex upon ion binding

Figs. 2 and 3 include the data on the responses of the emission intensity and the decay profile of the hybrid complex upon an addition of  $\text{NaClO}_4$  as a guest ion (G), respectively.

<sup>4</sup> The reduction and oxidation potentials of  $\text{RuB}_3^{2+}$  and  $\text{CS}^{4-}$  were  $-1.27$  and  $+1.00$  V (vs. SCE), respectively. The excited state energy of  $\text{RuB}_3^{2+}$  is 2.1 V, so that the Gibbs free energy change for PET between  $\text{RuB}_3^{2+}$  and  $\text{CS}^{4-}$  in methanol is calculated to be +0.4 kcal/mol.

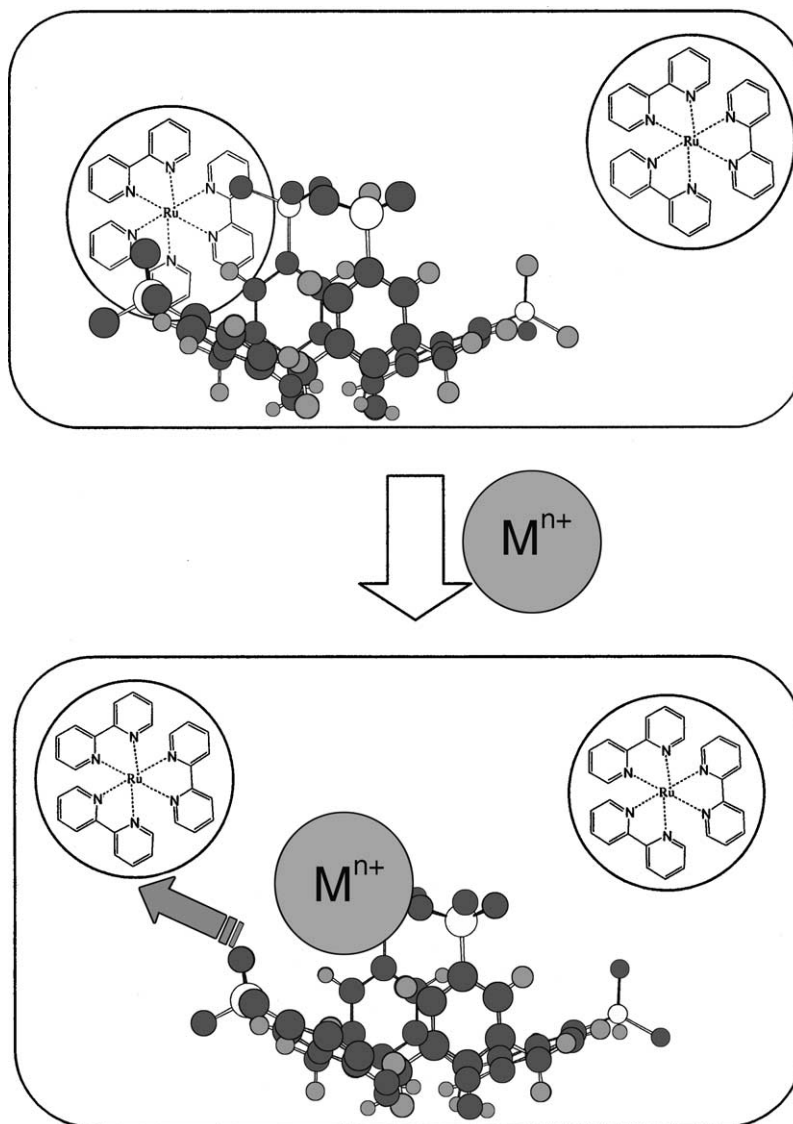


Fig. 4. Schematic illustrations of cation binding by a  $\text{CS}^{4-}:(\text{RuB}_3^{2+})_2$  hybrid complex in methanol.

As shown in Fig. 2, the emission intensity from the hybrid as a host (H) increased with an increase in the  $\text{NaClO}_4$  concentration ( $[\text{NaClO}_4]$ ). Furthermore, it is worth noting that the increase in the emission intensity accompanies a blue shift of the spectrum and, at  $[\text{NaClO}_4]:[\text{H}] = 5000:1$ , the maximum wavelength of the hybrid complex coincided with that of  $\text{RuB}_3^{2+}(\text{PF}_6^-)_2$  is 610 nm. As shown in Fig. 3, furthermore, the emission decay profile in the presence of  $\text{NaClO}_4$  was best fitted by the  $\tau_s = 390$  and  $\tau_1 = 720$  ns components with their amplitudes ( $A_s$  and  $A_1$ , respectively) being varied with  $[\text{NaClO}_4]$  (discussed later). At  $[\text{NaClO}_4]:[\text{H}] = 5000:1$ , the emission decay was best analyzed by a single exponential function with  $\tau_1 = 720$  ns, whose value was essentially the same with the emission lifetime of  $\text{RuB}_3^{2+}(\text{PF}_6^-)_2$  in methanol as described above. In the presence of  $\text{NaClO}_4$  as G, all the data indicate that  $\text{RuB}_3^{2+}$  in the hybrid complex is replaced by  $\text{Na}^+$ , leading to the increase in the mole

fraction of free  $\text{RuB}_3^{2+}$  not bound to  $\text{CS}^{4-}$ , as illustrated in Fig. 4. Besides  $\text{NaClO}_4$ , analogous experiments were conducted for  $\text{Bu}_4\text{NClO}_4$ ,  $\text{Mg}(\text{ClO}_4)_2$  and  $\text{Al}(\text{ClO}_4)_3$ , and we confirmed that the hybrid complex could sense a cation spectroscopically through the counter ion-exchange mechanism.

When H (hybrid complex) and G (cation) produces a 1:1 complex (Eq. (1))



the relevant equilibrium constant ( $K_a$ ) is given by Eq. (2), where  $[\text{H}]_0$  and  $[\text{G}]_0$  are the initial concentrations of H and G, respectively, and  $[\text{HG}]$  denotes the concentration of a host-guest complex.

$$K_a = \frac{[\text{HG}]}{[\text{H}][\text{G}]} = \frac{[\text{HG}]}{\{([\text{H}]_0 - [\text{HG}])([\text{G}]_0 - [\text{HG}])\}} \quad (2)$$

Under the assumption that the emission intensity from  $\text{RuB}_3^{2+}$  in the hybrid complex is proportional to the mole fraction of  $\text{RuB}_3^{2+}$ ,  $[\text{HG}]$  is expressed as in Eq. (3)

$$[\text{HG}] = [\text{H}]_0 \frac{I' - I_0}{I - I_0} \quad (3)$$

where  $I_0$ ,  $I$ , and  $I'$  are the emission intensities of H in the absence and presence of G, and that from the HG complex, respectively. According to the literature [10], we obtained Eq. (4)

$$\frac{I}{I_0} = 1 + \frac{I' - I_0}{I_0[\text{H}]_0} \times \left\{ \frac{[\text{G}]_0}{2} + \frac{\alpha}{2} \left[ 1 - \sqrt{\frac{[\text{G}]_0^2 - 2[\text{G}]_0\beta}{\alpha} + 1} \right] \right\} \quad (4)$$

where  $\alpha$  and  $\beta$  are defined as

$$\alpha = [\text{H}]_0 + K_a^{-1}, \quad \beta = [\text{H}]_0 - K_a^{-1}$$

The relationships between  $I/I_0$  determined at 610 nm and  $[\text{G}]$  obtained for four guest ions are summarized in Fig. 5. The  $[\text{G}]$  dependence of  $I/I_0$  was then fitted by Eq. (4) to evaluate the  $K_a$  value. As seen from the figure, the observed data were fitted almost satisfactorily with Eq. (4), indicating H:G = 1:1 complex formation. In order to confirm further the complexation behavior, the observed data were also analyzed by the Benesi–Hildebrand (BH) equation [11]. For H:G = 1:1 complex formation, the BH equation indicates that the inverse of the increment of the emission intensity ( $\Delta I^{-1}$ ) at a given  $[\text{G}]$  compared to  $I_0$  should linearly correlate with  $[\text{G}]^{-1}$ . As inserted in Fig. 5, indeed, we confirmed linear relationships between  $\Delta I^{-1}$  and  $[\text{G}]^{-1}$  for all guest

Table 1  
Association constants of H:G complexes determined by emission spectroscopy of the hybrid

	$K_a \times 10^{-3} \text{ M}^{-1}$	
	Emission intensity titration <sup>a</sup>	Emission lifetime titration <sup>b</sup>
$\text{NaClO}_4$	5.7	1.5
$\text{Bu}_4\text{NClO}_4$	7.2	1.8
$\text{Mg}(\text{ClO}_4)_2$	56	90
$\text{Al}(\text{ClO}_4)_3$	56	85

<sup>a</sup> Determined from the data in Fig. 5.

<sup>b</sup> Determined from the data in Fig. 6.

ions studied. The  $K_a$  values thus determined for four ions are listed in Table 1.

It is worth emphasizing that analogous analysis can be made on the basis of the emission decay data. Namely, since the  $A_1$  value ( $\tau_1 = 720 \text{ ns}$ ) corresponds to the mole fraction of dissociated  $\text{RuB}_3^{2+}$  from the hybrid complex in the presence of G as described above, the  $A_1$  value can be used instead of the  $I/I_0$  value in Eq. (4). Therefore, we conducted emission decay measurements of the hybrid in the presence of G, and the relationships between  $A_1$  and  $[\text{G}]$  for four G were determined as shown in Fig. 6. The best fits of the data by the analogous equation to Eq. (4) are included in Fig. 6 (solid curves). The  $K_a$  values determined by  $A_1$  are also shown in Table 1.

The  $K_a$  value determined from Fig. 6 for  $\text{Na}^+$  ( $1500 \text{ M}^{-1}$ ) was slightly smaller than that for  $\text{Bu}_4\text{N}^+$  ( $1800 \text{ M}^{-1}$ ), while that was  $\sim 5$  times larger for  $\text{Mg}^{2+}$  ( $90,000 \text{ M}^{-1}$ ) or  $\text{Al}^{3+}$  ( $85,000 \text{ M}^{-1}$ ). The sequence of the  $K_a$  value with G determined by the emission decay data ( $K_a$ :  $\text{Na}^+ \sim \text{TBA}^+ < \text{Mg}^{2+} \sim \text{Al}^{3+}$ ) agreed with that by emission intensity data

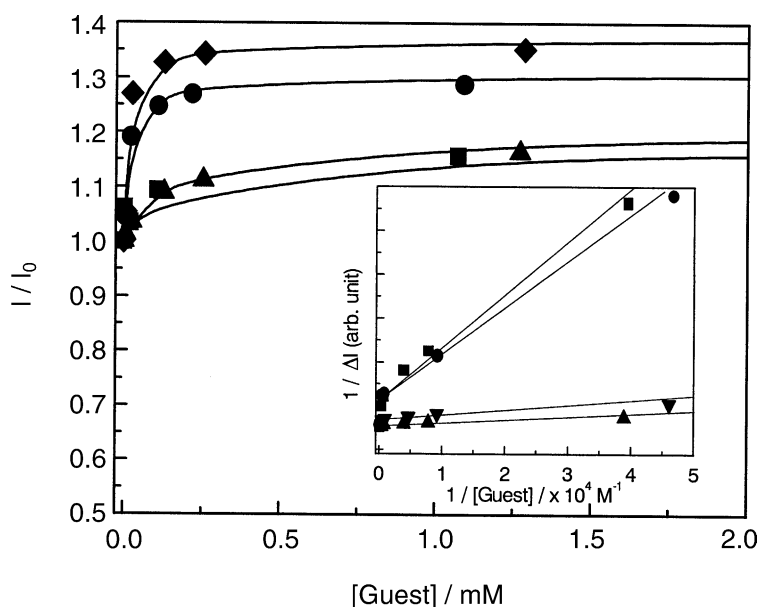


Fig. 5. Emission intensity (610 nm) responses of a  $\text{CS}_4^-:(\text{RuB}_3^{2+})_2$  hybrid complex ( $2.2 \times 10^{-6} \text{ M}$ ) in the presence of a guest cation ( $\text{Na}^+$  (▲),  $\text{Bu}_4\text{N}^+$  (■),  $\text{Mg}^{2+}$  (●) or  $\text{Al}^{3+}$  (◆)) in methanol (deaerated). Excitation wavelength is 355 nm. The inset represents Benesi–Hildebrand plots (see the main text).

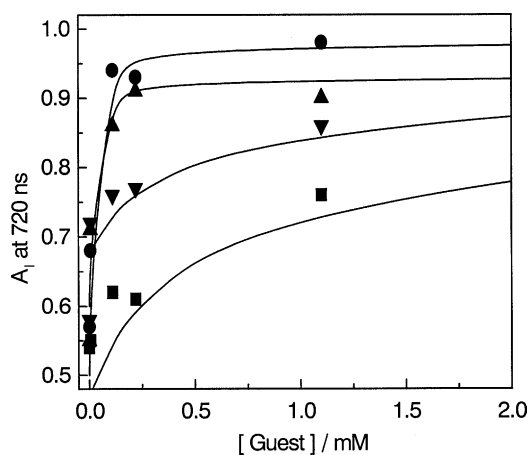


Fig. 6. Emission decay ( $A_1$ ) responses of a  $\text{CS}^{4-}:(\text{RuB}_3^{2+})_2$  hybrid complex ( $2.2 \times 10^{-6} \text{ M}$ ) in the presence of a guest cation ( $\text{Na}^+$  (▲),  $\text{Bu}_4\text{N}^+$  (■),  $\text{Mg}^{2+}$  (●) or  $\text{Al}^{3+}$  (◆)) in methanol (deaerated). Excitation and emission monitor wavelengths were set at 355 and 610 nm, respectively.

(Fig. 5), although the absolute values are somewhat different from each other (Table 1). It is worth noting that the values determined by  $I/I_0$  (Fig. 5) are not accurate enough, since the emission from the hybrid (H) exhibits the gradual spectral shift with the increase in  $[\text{G}]$  and, the emission intensity determined at a fixed wavelength (610 nm) does not necessarily correspond to the mole fraction of free  $\text{RuB}_3^{2+}$  (dissociated from the hybrid). On the other hand, since the emission decay measurements enable us separation of the mole fraction of free  $\text{RuB}_3^{2+}$  ( $A_1$ ) from the overall hybrid complex, we conclude that the  $K_a$  values determined by  $A_1$  are more reliable than those by  $I/I_0$ . Therefore, the discussion on  $K_a$  should be made on the basis of those obtained by  $A_1$  (Fig. 6).

The mono-valent cation of  $\text{Na}^+$  or  $\text{Bu}_4\text{N}^+$  gave the small  $K_a$  value ( $1500\text{--}1800 \text{ M}^{-1}$ ), while the di- or tri-valent cation showed the larger  $K_a$  value ( $85,000\text{--}90,000 \text{ M}^{-1}$ ). Since  $\text{RuB}_3^{2+}$  is di-valent, it is expected that two mono-valent guest ions are necessary to replace  $\text{RuB}_3^{2+}$  in the hybrid complex by G. Nonetheless, our data analysis by Eq. (4) or BH equation (Fig. 5) indicated H:G = 1:1 complexation, which demonstrates that association of one  $\text{Na}^+$  or  $\text{Bu}_4\text{N}^+$  ion to H is enough to release  $\text{RuB}_3^{2+}$  from the hybrid and charge compensation of  $\text{RuB}_3^{2+}(\text{ClO}_4^-)$  by another anion takes place successively in the solution phase. On the other hand, one  $\text{Mg}^{2+}$  or  $\text{Al}^{3+}$  ion is enough for releasing  $\text{RuB}_3^{2+}$  from the hybrid and simultaneous ion-exchange of the counter ions of  $\text{RuB}_3^{2+}$ , which would lead to the large  $K_a$  values for both  $\text{Mg}^{2+}$  and  $\text{Al}^{3+}$ . Since the present ion sensing is based on a counter ion-exchange reaction, the selectivity of the sensing is determined by the valency of a guest ion. Furthermore, the analogous  $K_a$  values between  $\text{Na}^+$  and  $\text{Bu}_4\text{N}^+$  or between  $\text{Mg}^{2+}$  and  $\text{Al}^{3+}$  demonstrate that the present results are not ascribed to simple ionic strength effects on the association–dissociation equilibrium of the hybrid complex in methanol. In the course of the present study,

Fiammengo et al. [12] reported separately  $\text{CS}^{4-}:\text{Zn}(\text{II})$  *meso*-tetrakis(*N*-alkylpyridinium-3-yl)porphyrin ion-pair complexes and demonstrated that the ion-pair complexes exhibited cation recognition abilities, similar to the present results, though their results on the  $K_a$  values towards guest ions are somewhat different from the present results owing to the difference in the composition of the hybrid. These results demonstrate that calix[4]arenetetrasulfonate is certainly very unique and easily functionalized by a desired cationic dye(s) ( $\text{D}^{m+}$ ). On the basis of a functionalized  $\text{CS}^{4-}:\text{D}^{m+}$  hybrid, various ions or molecules will be sensed by an appropriate method depending on  $\text{D}^{m+}$  introduced: UV absorption, luminescence, or electrochemical responses.

#### 4. Conclusions

We demonstrated spectroscopic and excited-state properties of a  $\text{CS}^{4-}:(\text{RuB}_3^{2+})_2$  hybrid complex as H, and the hybrid was successfully applied to cation sensing. On the basis of the emission dynamics of the hybrid complex, in particular, we succeeded in separating directly the mole fractions of G-bound (HG) and unbound hybrid (H) complexes and this enabled us to evaluate the association constant ( $K_a$ ) for cation sensing. Since the emission spectrum of free  $\text{RuB}_3^{2+}$  replaced by a guest cation(s) is superimposed to that of  $\text{CS}^{4-}:(\text{RuB}_3^{2+})_2$ , so that separation of these species from the spectrum is generally very difficult. In this respect, we think that the present photophysical approaches based on emission decay measurements are very potential for analyzing ion recognition behaviors. Calix[4]arenetetrasulfonate is easily derivatized by various dyes, so that the molecule could act as a potential chemosensor.

#### Acknowledgements

The authors are indebted to Dr. K. Tsuge and Prof. Y. Sasaki at Hokkaido University for their collaborations in X-ray measurements. NK thanks a Grant-in-aid from the Ministry of Education, Science, Sports, and Culture for the partial support of the research (No. 11440215).

#### References

- [1] C.D. Gutsche, Calixarenes Revisited: Monographs in Supramolecular Chemistry, Royal Society of Chemistry, Cambridge, UK, 1998.
- [2] A. Ikeda, S. Shinkai, Chem. Rev. 97 (1997) 1713.
- [3] P.D. Beer, F. Szemes, V. Balzani, C.M. Salà, M.G.B. Drew, S.W. Dent, M. Maestri, J. Am. Chem. Soc. 119 (1997) 11864.
- [4] D. Hasek, Y. Inoue, S.R.L. Everitt, M. Kunieda, H. Ishida, M.G.B. Drew, Tetrahedron-Asymmetry 9 (1998) 4089.
- [5] S. Shinkai, S. Mori, T. Tsubaki, T. Sone, O. Manabe, Tetrahedron Lett. 25 (1984) 5315.

- [6] K. Kalyanasundaram, *Photochemistry of Polypyridine and Porphyrin Complexes*, Academic Press, London, 1992.
- [7] W.J. Vinning, J.V. Casper, T.J. Meyer, *J. Phys. Chem.* 89 (1985) 1095.
- [8] E.M. Kober, B.P. Sullivan, T.J. Meyer, *Inorg. Chem.* 23 (1984) 2098.
- [9] J.V. Caspar, T.J. Meyer, *Inorg. Chem.* 22 (1983) 2444;  
J.V. Caspar, T.J. Meyer, *J. Am. Chem. Soc.* 105 (1983) 5583.
- [10] C.S. Wilcox, M.D. Cowart, J. Rebek Jr., *Tetrahedron Lett.* 27 (1986) 5563;  
H.-J. Schneider, R. Kramer, S. Simova, U. Schneider, *J. Am. Chem. Soc.* 110 (1988) 6442.
- [11] R.S. Mulliken, *Molecular Complexes*, Wiley/Interscience, New York, 1969.
- [12] R. Fiammengo, P. Timmerman, F. De Jong, D.N. Reinhoudt, *Chem. Comm.* 2313 (2000).